

Extraction of Nonlinear Thermo-Electroelastic Equations for High Frequency Vibrations of Piezoelectric Resonators with Initial Static Biases

M. M. Mohammadi ^{1,*}, M. Hamedi ², H. Daneshpajoo ³

¹*School of Mechanical Engineering, College of Engineering, University of Zanjan, Zanjan, Iran*

²*College of Mechanical Engineering, University of Tehran, Tehran, Iran*

³*Department of Electrical Engineering, Pennsylvania State University, USA*

Received 7 June 2018; accepted 7 August 2018

ABSTRACT

In this paper, the general case of an anisotropic thermo-electro elastic body subjected to static biasing fields is considered. The biasing fields may be introduced by heat flux, body forces, external surface tractions, and electric fields. By introducing proper thermodynamic functions and employing variational principle for a thermo-electro elastic body, the nonlinear constitutive relations and the nonlinear equation of motion are extracted. The equations have the advantage of employing the Lagrangian strain and second Piola-Kirchhoff stress tensor with symmetric characteristics. These equations are used to analyze the high frequency vibrations of piezoelectric resonators under finite biasing fields. A system of three dimensional equations is derived for initial and incremental fields on the body. Capability of the equations in numerical modelling of temperature-frequency and force-frequency effects in quartz crystal is demonstrated. The numerical results compare well with the data from experiments. These equations may be used in accurate modelling of piezoelectric devices subjected to thermo electro mechanical loads.

© 2018 IAU, Arak Branch. All rights reserved.

Keywords : Nonlinear equations, Thermo-electro elasticity, Initial static bias, Resonators.

1 INTRODUCTION

A piezoelectric resonator usually consists of a piezoelectric crystal equipped with one or more pair of conducting metallic electrodes [1]. When the resonator is subjected to external forces, acceleration, temperature change, and electric fields, its resonance frequency is changed. These conditions may lead to instabilities of oscillator circuits in the electronic devices. Accurate modelling of such environmental effects is essential for the design of stable resonators. This problem belongs to the general theory of incremental elastic deformations superposed on initial finite deformation [2]. When a solid body is free of initial stresses, the linear theory of elasticity can accurately describe the propagation of small amplitude acoustic waves in the body. However, when the solid is subject to biasing stresses or strains, the linear theory of elasticity cannot explain the response of the solid to the propagation of small elastic waves. This is primarily due to the fact that, at this state, the small increment of stress is a function of both infinitesimal increment in local rotation and strain [3]. On the other hand, the shape and size of

*Corresponding author.

E-mail address: dr.mohamamdi@gmail.com (M.M.Mohammadi).

the body are changed by the application of the biasing fields. Therefore, all quantities referred to unit volume or unit area, such as Cauchy stress tensor, are influenced by the continuous change of the volume and surface area. These geometrical nonlinearities result in a deviation from truly linear behavior [4]. For compensating the geometrical nonlinearities in calculations, Lagrangian description can be used. In Lagrangian description, the field variables are coordinates of material points in the reference frame. In the reference frame, the material is free of any strain or stress, and it has a constant reference temperature [5]. The convenient stress tensors to be used in Lagrangian description are the first and second Piola-Kirchhoff stress tensors. These stress tensors are referred to a material surface in the reference configuration. Employing these two different stress tensors results in two different sets of equations governing the problem of small fields superposed on static biases. The second Piola-Kirchhoff stress tensor is symmetric while the first one is not.

Some researchers have employed the first Piola-Kirchhoff stress tensors for analyzing the high frequency vibrations of piezoelectric materials under biasing fields. For example, Tiersten et al. explained the behavior of an electrically polarizable, finitely deformable, heat conducting continuum, in interaction with the electric field. They introduced a convenient energy function which is scalar invariant under rigid rotations of the deformed and polarized body [6]. In other papers, Tiersten et al. derived nonlinear thermo-electro elastic equations, including quadratic and cubic terms of small field variables for electro elastic bodies [3, 7]. Yong derived the nonlinear equations for small fields superposed on initial biases in thermo-electro elastic bodies. Free vibrations of a linear thermo-piezoelectric body were analyzed by Yong and Batra [8]. Other researchers employed the second Piola-Kirchhoff stress tensor in their analysis. Among them is Lee who developed a systematic method for calculation of the frequency shift in piezoelectric resonators subject to initial mechanical biases [9]. In another work, Lee and Yong extracted the linear field equations for small vibrations superposed on thermally-induced deformations from the nonlinear field equations of the thermo-elasticity in Lagrangian formulation. The initial deformations were introduced due to the steady and uniform temperature changes [10]. Yong and Wei revisited the work of Lee and involved the piezoelectric effects in their calculations [11]. Wang et al. calculated the frequency shift of a piezoelectric resonator subject to initial mechanical biases [12]. They considered the piezoelectricity in their formulations. Effects of thermal stresses on the frequency-temperature behavior of piezoelectric resonators were analyzed by Yong et al. They employed the Lagrangian equations for small incremental displacements superposed on initial thermal stresses and strains. In their work, the temperature derivatives of the material constants were incorporated in the constitutive equations for the incremental displacements [13].

The review of the literature reveals that the governing nonlinear thermo-electro elastic equations, incorporating the second Piola-Kirchhoff stress tensors, have not been developed for the problem of small fields superposed on static biases. The aim of this paper is to extract these equations using convenient energy functions. In the first part of the paper, the general case of a piezo- and/or pyro-electric body subjected to a finite biasing field is considered. By employing two different third order electric Gibbs function, the second Piola-Kirchhoff stress tensors, electric polarization vector, electric displacement vector, and entropy per unit mass are obtained as a function of Lagrangian strain, temperature, and electric field. Moreover, by using generalized Hamilton's principle the equation of motion is extracted. In the second part of the paper, by employing the derived equations, the equations governed for the initial, and final state, and for the incremental fields in a piezoelectric resonator subjected to biasing fields are obtained. In the final part, the response of a quartz resonator to homogenous thermal and mechanical biases is investigated. The force frequency effect in quartz resonator at 78°C is numerically modeled for the first time.

2 THE GOVERNING EQUATIONS

Consider the general case of a piezoelectric body subjected to temperature change, body force, external surface traction, and electric field. Due to these biasing fields, the position of a material point is moved from X_I to y_I (as seen in Fig. 1). Hence, the displacement vector and the nonlinear Lagrangian strain are yield in the reference frame as Eqs. (1)-(2) [14, 15].

$$U_I = y_I - X_I, \quad (1)$$

$$S_{IJ} = \frac{1}{2}(U_{I,J} + U_{J,I} + U_{K,I}U_{K,J}), \quad (2)$$

where, $U_{i,j} = \frac{\partial U_i}{\partial X_j}$. For the electric field, by using Maxwell's equations, we have: [16]

$$W_i = -\varphi_{,i} \tag{3}$$

where, W is the electric field intensity, and φ is the scalar electric potential at the initial state.

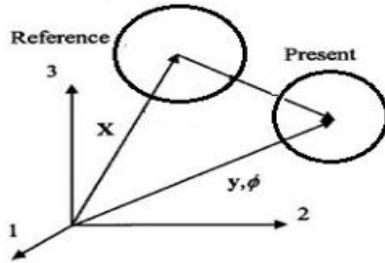


Fig.1 Deformation of a thermo-electro elastic body.

According to the principle of conservation of energy for a piezoelectric medium with volume V , surface S , and with unit normal vector n , the rate of the energy increase equals to the rate at which work is done by the surface traction acting on S minus the outward heat flux from the body to the environment [6, 17]. This concept is represented in (4).

$$\frac{d}{dt} \int_V \rho \left(\frac{1}{2} v_i v_i + \epsilon \right) dV = \int_S (t_i^M v_i - n_i q_i) dS + \int_V \rho \frac{d}{dt} (\Pi_i W_i dV + \int_V B_i v_i dV, \tag{4}$$

where, ρ is the density, ϵ is the internal energy per unit mass, $v_i = dy_i / dt$, t_i^M is the mechanical surface traction, $n_i q_i$ is the rate of outward flux of thermal energy per unit area, Π is the electric polarization per unit mass, and B is the body force. By applying the divergence theorem and Cauchy stress principle ($t_j^M = n_i \tau_{ij}$), and transforming the tensorial parameters to the reference frame, Eq. (4) can be expressed as: [5]

$$\rho_0 \frac{d\epsilon}{dt} = T_{LM} \frac{dS_{LM}}{dt} + \rho_0 \frac{dp_L}{dt} W_L + \rho_0 \theta \frac{d\eta}{dt} \tag{5}$$

where, $\rho_0, T_{LM}, S_{LM}, p_L, W_L, \theta$, and η are the initial density of the body, second Piola-Kirchhoff stress tensor, Lagrangian strain tensor, electric polarization, electric field intensity, absolute temperature, and entropy per unit mass, respectively. All these quantities are calculated at the reference frame. In obtaining the Eq. (5), the following relations are used: [5]

$$\begin{aligned} y_{j,L} &= \frac{\partial y_j}{\partial X_L} \\ S_{LM} &= y_{j,L} y_{j,M} - \delta_{LM} \\ p_K &= \rho_0 X_{K,i} \Pi_i \\ \tau_{ij} &= \frac{1}{J} y_{i,L} T_{LM} y_{j,M} - \rho \Pi_i E_j \\ W_L &= y_{k,L} W_k = -\varphi_{,L} \\ J &= \frac{\rho_0}{\rho} = \det(y_{i,L}) \end{aligned} \tag{6}$$

where, J is the Jacobian of deformation, and τ_{ij} is the cauchy stress tensor. According to the Eq. (5), the thermodynamic function, ϵ , may be expressed as:

$$\epsilon = \epsilon(S_{LM}, p_K, \eta) \quad (7)$$

According to the principle of material objectivity, defining the thermodynamic function, ϵ , as Eq. (7), makes it a scalar quantity which is invariant under rigid rotation of the deformed and polarized body [6].

2.1 Gibbs electric energy

Since the aim of this paper is to analyze the behavior of piezoelectric material subjected to the temperature change and electric fields, it is more convenient to define the electric Gibbs function χ which depends on the temperature and electric field. By using the Legendre transformation, we can define this function as: [5]

$$\chi = \epsilon - \eta\theta - W_L p_L \quad (8)$$

By employing Eq. (5), the Eq. (8) can be rewritten as:

$$\rho_0 \frac{d\chi}{dt} = T_{LM} \frac{dS_{LM}}{dt} - \rho_0 \frac{dW_L}{dt} p_L - \rho_0 \frac{d\theta}{dt} \eta \quad (9)$$

Then, we have:

$$\chi = \chi(S_{LM}, W_L, \theta) \quad (10)$$

Due to the fact that the variation of temperature, mechanical strain, and electric potential is finite, the variation of electric Gibbs function, χ , can be obtained using the second and third order terms of the Taylor's expansion. The expansion of electric Gibbs function around the state $(E, W, \theta) = (0, 0, \theta_0)$, up to the third order may be written as:

$$\begin{aligned} \chi(S, W, \theta) = & \frac{1}{2} \left[\frac{\partial^2 \chi}{\partial S^2} \Big|_{0,0,\theta_0} \times S^2 + 2 \frac{\partial^2 \chi}{\partial S \partial W} \Big|_{0,0,\theta_0} \times SW + 2 \frac{\partial^2 \chi}{\partial S \partial \theta} \Big|_{0,0,\theta_0} \times S(\theta - \theta_0) + \frac{\partial^2 \chi}{\partial W^2} \Big|_{0,0,\theta_0} \times W^2 + \right. \\ & 2 \frac{\partial^2 \chi}{\partial W \partial \theta} \Big|_{0,0,\theta_0} \times W(\theta - \theta_0) + \left. \frac{\partial^2 \chi}{\partial \theta^2} \Big|_{0,0,\theta_0} \times (\theta - \theta_0)^2 \right] + \frac{1}{6} \left[\frac{\partial^3 \chi}{\partial S^3} \Big|_{0,0,\theta_0} \times S^3 + 3 \frac{\partial^3 \chi}{\partial S^2 \partial W} \Big|_{0,0,\theta_0} \times S^2 W + \right. \\ & 3 \frac{\partial^3 \chi}{\partial S^2 \partial \theta} \Big|_{0,0,\theta_0} \times S^2(\theta - \theta_0) + 3 \frac{\partial^3 \chi}{\partial S W^2} \Big|_{0,0,\theta_0} \times S W^2 + 3 \frac{\partial^3 \chi}{\partial E \partial \theta^2} \Big|_{0,0,\theta_0} \times S(\theta - \theta_0)^2 + \\ & 6 \frac{\partial^3 \chi}{\partial S \partial W \partial \theta} \Big|_{0,0,\theta_0} \times S W(\theta - \theta_0) + \frac{\partial^3 \chi}{\partial W^3} \Big|_{0,0,\theta_0} \times W^3 + 3 \frac{\partial^3 \chi}{\partial W^2 \partial \theta} \Big|_{0,0,\theta_0} \times W^2(\theta - \theta_0) + \\ & \left. 3 \frac{\partial^3 \chi}{\partial W \partial \theta^2} \Big|_{0,0,\theta_0} \times W(\theta - \theta_0)^2 + \frac{\partial^3 \chi}{\partial \theta^3} \Big|_{0,0,\theta_0} \times (\theta - \theta_0)^3 \right] \quad (11) \end{aligned}$$

The coefficients in Eq. (11) are the isothermal fundamental material constants of the piezoelectric medium. Thus, Eq. (11) may be written in the tensorial form as:

$$\begin{aligned}
 \rho\chi(S, W, \theta) = & \chi(0, 0, \theta_0) + \frac{1}{2}C_{IJKL} \times S_{IJ}S_{KL} - e_{LJP} \times S_{IJ}W_P - \beta_{LJ} \times S_{LJ} (\theta - \theta_0) - \\
 & \frac{1}{2}x_{PQ} \times W_PW_Q - \lambda_p \times W_P (\theta - \theta_0) - \frac{1}{2}\kappa \times (\theta - \theta_0)^2 + \frac{1}{6}C_{IJKLMN} \times S_{IJ}S_{KL}S_{MN} + \\
 & \frac{1}{2}d_{IJKLP} \times S_{IJ}S_{KL}W_P + \frac{1}{2}\frac{\partial C_{IJKL}}{\partial \theta} \times S_{IJ}S_{KL} (\theta - \theta_0) - \frac{1}{2}b_{LJPQ} \times S_{LJ}W_PW_Q - \\
 & \frac{1}{2}\frac{\partial \beta_{LJ}}{\partial \theta} \times S_{LJ} (\theta - \theta_0)^2 - \frac{1}{2}\frac{\partial e_{LJP}}{\partial \theta} \times S_{LJ}W_P (\theta - \theta_0) - \frac{1}{6}x_{PQR} \times W_PW_QW_R - \\
 & \frac{1}{2}\frac{\partial x_{PQ}}{\partial \theta} \times W_PW_Q (\theta - \theta_0) - \frac{1}{2}\frac{\partial \lambda_p}{\partial \theta} \times W_P (\theta - \theta_0)^2 - \frac{1}{6}\frac{\partial \kappa}{\partial \theta} \times (\theta - \theta_0)^3.
 \end{aligned}
 \tag{12}$$

Table 1. demonstrates the name of material constants in the Eq. (12). All the coefficients are measured at the temperature θ_0 , when the body is free of strain and electric field.

Table 1

The fundamental material constants.

C_{IJKL}	Second order elastic constant
C_{IJKLMN}	Third order elastic constant
$\frac{\partial C_{IJKL}}{\partial \theta}$	First temperature derivative of second order elastic constant
e_{LJP}	Piezoelectric constant
$\frac{\partial e_{LJP}}{\partial \theta}$	First temperature derivative of piezoelectric constant
β_{LJ}	Thermo-elastic constant
$\frac{\partial \beta_{LJ}}{\partial \theta}$	First temperature derivative of thermoelastic constant
x_{IJ}	Second order electric permeability
x_{LJP}	Third order electric permeability
$\frac{\partial x_{IJ}}{\partial \theta}$	First temperature derivative of second order electric permeability
λ_i	Pyroelectric constant
$\frac{\partial \lambda_i}{\partial \theta}$	First temperature derivative of Pyroelectric constant
κ	A coefficient related to the specific heat
$\frac{\partial \kappa}{\partial \theta}$	First temperature derivative of κ
d_{IJKLP}	First odd electro elastic constant
b_{LJPQ}	Electrostrictive constant

The material constants presented in Table 1. are called the fundamental material constants [17, 4].

2.2 Other form of the electric Gibbs energy

The term of electric energy in Eq. (4) can be expressed in terms of the product of electric displacement and electric field. Accordingly, the law of conservation of energy may be written in the form of: [1]

$$\frac{d}{dt} \int_V (\rho \frac{1}{2} v_i v_i + U) dV = \int_S (t_i^M v_i - n_i q_i) dS + \int_V \frac{d}{dt} (D_i) \mathcal{W}_i dV + \int_V b_i v_i dV, \quad (13)$$

In which, U is the internal energy. Following a similar procedure as stated above, for the internal energy in the reference frame, we may have:

$$U = U(S_{LM}, \Delta_L, \eta) \quad (14)$$

where, Δ is the material form of D in the reference frame that may be obtained by:

$$\Delta_L = J \frac{\partial X_L}{\partial y_j} D_j \quad (15)$$

Consequently, we have:

$$\rho_0 \frac{dU}{dt} = T_{LM} \frac{dS_{LM}}{dt} + \frac{d\Delta_L}{dt} W_L + \rho_0 \theta \frac{d\eta}{dt} \quad (16)$$

By employing the Legendre transformation, we can define the electric Gibbs function as:

$$\psi = U - \eta\theta - W_L \Delta_L \quad (17)$$

which results in:

$$\rho_0 \frac{d\psi}{dt} = T_{LM} \frac{dS_{LM}}{dt} - \frac{dW_L}{dt} \Delta_L - \rho_0 \frac{d\theta}{dt} \eta. \quad (18)$$

Finally, we have:

$$\psi = \psi(S_{LM}, W_L, \theta) \quad (19)$$

Similar to Eq. (12), the thermodynamic potential, ψ , can be represented by a generalized Taylor's expansion in terms of the independent variables (S_{LM}, W_L, θ) . The potential function, ψ , may be written as:

$$\begin{aligned} \rho_0 \psi(S, W, \theta) = & + \frac{1}{2} C_{LKl} \times S_{Ll} S_{KL} - e_{lP} \times S_{Ll} W_P - \beta_{Ll} \times S_{Ll} (\theta - \theta_0) - \\ & \frac{1}{2} \varepsilon_{PQ} \times W_P W_Q - \lambda_P \times W_P (\theta - \theta_0) - \frac{1}{2} \kappa \times (\theta - \theta_0)^2 + \frac{1}{6} C_{LKLmn} \times S_{Ll} S_{KL} S_{MN} + \\ & \frac{1}{2} d_{LKLp} \times S_{Ll} S_{KL} W_P + \frac{1}{2} \frac{\partial C_{LKl}}{\partial \theta} \times S_{Ll} S_{KL} (\theta - \theta_0) - \frac{1}{2} b_{LlPQ} \times S_{Ll} W_P W_Q - \\ & \frac{1}{2} \frac{\partial \beta_{Ll}}{\partial \theta} \times S_{Ll} (\theta - \theta_0)^2 - \frac{1}{2} \frac{\partial e_{lP}}{\partial \theta} \times S_{Ll} W_P (\theta - \theta_0) - \frac{1}{6} \varepsilon_{PQR} \times W_P W_Q W_R - \\ & \frac{1}{2} \frac{\partial \varepsilon_{PQ}}{\partial \theta} \times W_P W_Q (\theta - \theta_0) - \frac{1}{2} \frac{\partial \lambda_P}{\partial \theta} \times W_P (\theta - \theta_0)^2 - \frac{1}{6} \frac{\partial \kappa}{\partial \theta} \times (\theta - \theta_0)^3. \end{aligned} \quad (20)$$

By considering the thermodynamic potential, ψ the second and third order dielectric permittivity ($\varepsilon_{PQ}, \varepsilon_{PQR}$) are defined. Employing the potential functions, ψ and χ , the thermodynamic tension or second Piola-Kirchhoff stress tensors, electric polarization, entropy, and electric displacement are obtained as [21]:

$$\begin{aligned}
 T_{KL} &= \rho_0 \left. \frac{\partial \chi}{\partial S_{KL}} \right|_{W, \theta} = \rho_0 \left. \frac{\partial \psi}{\partial S_{KL}} \right|_{W, \theta} \\
 p_K &= -\rho_0 \left. \frac{\partial \chi}{\partial W_K} \right|_{E, \theta}, \\
 \eta &= -\rho_0 \left. \frac{\partial \chi}{\partial \theta} \right|_{W, E} = -\rho_0 \left. \frac{\partial \psi}{\partial \theta} \right|_{W, E}. \\
 \Delta_k &= -\rho_0 \left. \frac{\partial \psi}{\partial W_K} \right|_{W, E}
 \end{aligned}
 \tag{21}$$

Substituting Eqs. (12) and (20) in the (21) results in:

$$\begin{aligned}
 T_{LJ} &= \left[C_{LJKL} + \frac{1}{2} C_{LJKLMN} \times S_{MN} + d_{LJKLP} \times W_P + \frac{\partial C_{LJKL}}{\partial \theta} \times (\theta - \theta_0) \right] S_{KL} - \\
 &\left[e_{LJP} + \frac{1}{2} \frac{\partial e_{LJP}}{\partial \theta} \times (\theta - \theta_0) + \frac{1}{2} b_{LJPQ} \times W_Q - d_{LJKLP} \times S_{KL} \right] W_P - \left[\beta_{LJ} + \frac{1}{2} \frac{\partial \beta_{LJ}}{\partial \theta} \times (\theta - \theta_0) \right] \times (\theta - \theta_0), \\
 P_P &= \left[e_{LJP} - \frac{1}{2} d_{LJKLP} \times S_{KL} + b_{LJPQ} \times W_Q + \frac{1}{2} \frac{\partial e_{LJP}}{\partial \theta} \times (\theta - \theta_0) \right] S_{LJ} \\
 &+ \left[x_{PQ} + \frac{1}{2} x_{PQQR} \times W_R + \frac{\partial x_{PQ}}{\partial \theta} \times (\theta - \theta_0) \right] W_Q + \left[\lambda_p + \frac{1}{2} \frac{\partial \lambda_p}{\partial \theta} \times (\theta - \theta_0) \right] (\theta - \theta_0), \\
 \eta &= \left[\beta_{LJ} + \frac{\partial \beta_{LJ}}{\partial \theta} \times (\theta - \theta_0) - \frac{1}{2} \frac{\partial C_{LJKL}}{\partial \theta} \times S_{KL} + \frac{1}{2} \frac{\partial e_{LJP}}{\partial \theta} \times W_P \right] \times S_{LJ} - \\
 &\left[\lambda_p + \frac{1}{2} \frac{\partial \lambda_p}{\partial \theta} \times W_Q + \frac{\partial \lambda_p}{\partial \theta} \times (\theta - \theta_0) \right] \times W_P + \left[\kappa + \frac{\partial \kappa}{\partial \theta} \times (\theta - \theta_0) \right] \times (\theta - \theta_0), \\
 \Delta_p &= \frac{\partial \psi}{\partial W_P} = \left[e_{LJP} + \frac{1}{2} \frac{\partial e_{LJP}}{\partial \theta} \times (\theta - \theta_0) - \frac{1}{2} d_{LJKLP} \times S_{KL} + b_{LJPQ} \times W_Q \right] \times S_{LJ} + \\
 &\left[\varepsilon_{PQ} + \frac{\partial \varepsilon_{PQ}}{\partial \theta} \times (\theta - \theta_0) + \frac{1}{2} \varepsilon_{PQQR} \times W_R \right] \times W_Q + \left[\lambda_p + \frac{1}{2} \frac{\partial \lambda_p}{\partial \theta} \times (\theta - \theta_0) \right] \times (\theta - \theta_0).
 \end{aligned}
 \tag{22}$$

2.3 Equation of motion

The generalized Hamilton's principle has the form of (23):

$$\delta \int_{t_1}^{t_2} (K - F) dt = 0,
 \tag{23}$$

where K and F are the kinetic energy and potential functions which can be obtained by: [18, 19]

$$F = \int_{V_0} (\rho_0 \psi + \rho_0 \eta \theta - B_I U_I) dV - \int_{S_0} (T_I^M U_I - \Sigma \phi) dS,
 \tag{24}$$

and

$$F = \int_{V_0} (\rho_0 \psi + \rho_0 \eta \theta - B_I U_I) dV - \int_{S_0} (T_I^M U_I - \Sigma \phi) dS,
 \tag{25}$$

where, T_I^M , B_I , and Σ respectively are the surface traction, body force, and surface charge density in the reference configuration. Substituting Eqs. (24) and (25) into (23), and considering Eq. (6), the following relation is obtained:

$$\delta \int_{t_1}^{t_2} (K - F) dt = \int_{V_0} [(-\rho_0 \ddot{U}_I + (T_{LJ} + T_{KJ} U_{I,K})_{,J} + B_I) \delta U_I + \Delta_{I,I} \delta \varphi] + \int_{S_0} (T_I^M \delta U_I + \Sigma \delta \varphi - \Delta_I N_I \delta \varphi - T_{LJ} \delta U_I N_J - T_{KJ} U_{I,K} \delta U_I N_J) dS = 0 \quad (26)$$

Eq. (26) leads to the following governing equations and initial conditions:

$$\begin{aligned} (T_{LJ} + T_{KJ} U_{I,K})_{,J} + B_I &= \rho_0 \ddot{U}_I \\ \Delta_{I,I} &= 0, \\ T_I^M &= (T_{LJ} + T_{KJ} U_{I,K}) N_J, \\ \Sigma &= \Delta_I N_I. \end{aligned} \quad (27)$$

where, N_i is the unit outward normal on the undeformed body. The extracted equation of motion is similar to the equation of motion for a crystal under pure mechanical biases [10]. It can be concluded that the thermal biases do not change the form of the equation of motion. However, the initial thermal biases change the values of initial stresses and displacement gradients.

3 VIBRATION OF RESONATORS UNDER BIASING FIELDS

The theory of small fields superposed on finite static bias in a piezoelectric resonator can only be obtained from the fully nonlinear theory of thermoelectroelasticity [20]. In this theory, three states are considered for the piezoelectric body (see Fig. 2).

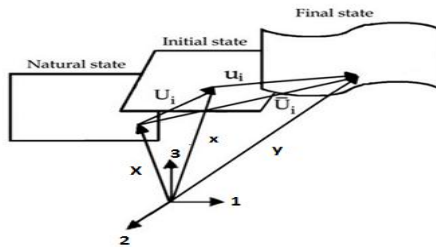


Fig.2
Three states of the piezoelectric resonator.

Natural state

At the natural state, the material is at rest and free of stress and strain, and has a uniform temperature θ_0 . A generic point at this state is denoted by the Cartesian coordinate of X_i .

Initial state

At the initial state, the body is subjected to thermal, mechanical, and/or electrical deformations. The temperature changes uniformly and steadily from θ_0 to θ . The external forces are applied to the boundary of the body. Electrical DC bias can be employed to the electrodes. This condition leads to occurrence of a finite and static deformation on the piezoelectric body, and the position of a material point is moved, due to static deformation, from X_i to x_i .

Final state

At this state, adiabatic small vibrations are superposed on the deformed body. The temperature change can be assumed negligible. [10] As a result of small vibrations, the position of a material point is moved from x_i to y_i . Due to the infinitesimal deformations in the final state, it is possible to obtain the final state of the body by solving a set of linear partial differential equations [20].

3.1 Governing equations for the final and initial state

At the final state, the small amplitude vibrations are superposed on thermally and mechanically induced deformations occurred in the initial state. The position of a generic material point is moved from x_i to y_i . Thus, the displacement vector is $u_i = y_i - x_i$ which is called the incremental displacement. As shown in Fig. 2, the total displacement from the natural state to the final state can be obtained by:

$$\bar{U}_i = y_i - X_i = U_i + u_i. \tag{28}$$

where, \bar{U}_i is the displacement vector at the final state. Similarly, for the electric potential, surface traction, and body force, we have: [8]

$$\begin{aligned} \bar{\varphi} &= \varphi^0 + \varphi^1, \\ \bar{T}_I^M &= T_I^M + \tau_I^M, \\ \bar{B}_I &= B_I + b_I, \\ \bar{\Delta}_I &= \Delta_I + d_I. \end{aligned} \tag{29}$$

where, $\varphi^1, \tau_I^M, \beta_i$, and d_i are the incremental electric potential, surface traction, body force, and electric displacement, respectively. The barred and unbarred uppercase quantities are related to the final state and the initial fields, respectively [12, 20]. In the previous section, the governing equations for a body subjected to finite biasing fields were extracted. Accordingly, the governing equations for the final state of the resonator are:

$$\begin{aligned} \bar{S}_{IJ} &= \frac{1}{2}(\bar{U}_{I,J} + \bar{U}_{J,I} + \bar{U}_{K,I}\bar{U}_{K,J}), \\ \bar{W}_L &= -\bar{\varphi}_{,L}, \\ \bar{T}_{IJ} &= \left[C_{LKl} + \frac{1}{2}C_{LKLmn} \times \bar{S}_{mn} + d_{LKLp} \times \bar{W}_p + \frac{\partial C_{LKl}}{\partial \theta} \times (\theta - \theta_0) \right] \bar{S}_{kl} - \\ &\left[e_{lp} + \frac{1}{2} \frac{\partial e_{lp}}{\partial \theta} \times (\theta - \theta_0) + \frac{1}{2} b_{lpq} \times \bar{W}_q - d_{LKLp} \times \bar{S}_{kl} \right] \bar{W}_p - \left[\beta_{lj} + \frac{1}{2} \frac{\partial \beta_{lj}}{\partial \theta} \times (\theta - \theta_0) \right] \times (\theta - \theta_0), \\ \bar{\Delta}_p &= \left[e_{lp} + \frac{1}{2} \frac{\partial e_{lp}}{\partial \theta} \times (\theta - \theta_0) - \frac{1}{2} d_{LKLp} \times \bar{S}_{kl} + b_{lpq} \times \bar{W}_q \right] \times \bar{S}_{lj} + \\ &\left[\varepsilon_{pq} + \frac{\partial \varepsilon_{pq}}{\partial \theta} \times (\theta - \theta_0) + \frac{1}{2} \varepsilon_{pqr} \times \bar{W}_r \right] \times \bar{W}_q + \left[\lambda_p + \frac{1}{2} \frac{\partial \lambda_p}{\partial \theta} \times (\theta - \theta_0) \right] \times (\theta - \theta_0). \end{aligned} \tag{30}$$

and

$$\begin{aligned} (\bar{T}_{IJ} + \bar{T}_{JK}\bar{U}_{I,K})_{,J} + \rho_0 \bar{B}_I &= \rho_0 \ddot{\bar{U}}_I, \\ \bar{\Delta}_{I,I} &= 0, \\ \bar{T}_I^M &= n_J (\bar{T}_{IJ} + \bar{T}_{JK}\bar{U}_{I,K}), \\ \bar{\Sigma} &= N_I \bar{\Delta}_I, \end{aligned} \tag{31}$$

For obtaining the third and fourth equation of (30), it is assumed that the temperature variation resulted from the incremental displacement was negligible [10].

3.2 The governing equations for the initial state

Since material properties remain unchanged during the thermal expansion and the incremental vibrations, the governing equations of the initial state are the same as Eqs. (30), (31) of the final state. Thus, to obtain the equations of the initial state, it is sufficient to replace the barred quantities of Eqs. (30), (31) with unbarred quantities. However, due to the static deformation in the initial state, the equation of motion should be changed to:

$$(T_{IJ} + T_{JK}U_{I,K})_{,J} + \rho_0 B_I = 0 \quad (32)$$

3.3 The governing equation for the incremental fields

By taking the difference between the corresponding field equations in the final and initial states, a set of linear equations for small amplitude vibrations superposed on finite biases are obtained. Accordingly, the incremental Lagrangian strain is expressed by:

$$s_{IJ} = \frac{1}{2}(u_{I,J} + u_{J,I} + U_{K,I}u_{K,J} + u_{K,I}U_{K,J}), \quad (33)$$

and, we have $s_{IJ} = \bar{S}_{IJ} - S_{IJ}$. For the electric field we have:

$$\bar{W}_L = -\bar{\varphi}_{,L} = -(\varphi^0 + \varphi^1)_{,L} = -\varphi_{,L}^0 - \varphi_{,L}^1 = W_L + w_L \quad (34)$$

where, w_L is the incremental electric field. By inserting the initial and incremental strains and electric fields into the third equation of (30), and neglecting the small incremental temperature change [10], the final stress may be written as:

$$\begin{aligned} \bar{T}_{IJ} = & \left[C_{LJKL} + \frac{\partial C_{LJKL}}{\partial \theta} (\theta - \theta_0) + \frac{1}{2} C_{LJKLMN} S_{MN} \right] S_{KL} + \left[C_{LJKL} + \frac{\partial C_{LJKL}}{\partial \theta} (\theta - \theta_0) + C_{LJKLMN} S_{MN} + d_{LJKLP} W_P \right] s_{KL} \\ & - \left[e_{LJP} + \frac{1}{2} b_{LJPQ} W_Q + \frac{1}{2} \frac{\partial e_{LJP}}{\partial \theta} (\theta - \theta_0) - d_{LJKLP} \times S_{KL} \right] W_P - \left[e_{LJP} + b_{LJPQ} W_Q + \frac{1}{2} \frac{\partial e_{LJP}}{\partial \theta} (\theta - \theta_0) - d_{LJKLP} S_{KL} \right] w_P. \end{aligned} \quad (35)$$

where, t_{ij} is the incremental stress, and we have:

$$\begin{aligned} t_{IJ} = & \left[C_{LJKL} + \frac{\partial C_{LJKL}}{\partial \theta} (\theta - \theta_0) + C_{LJKLMN} S_{MN} + d_{LJKLP} W_P \right] s_{KL} - \\ & \left[e_{LJP} + b_{LJPQ} W_Q + \frac{1}{2} \frac{\partial e_{LJP}}{\partial \theta} (\theta - \theta_0) - d_{LJKLP} S_{KL} \right] w_P \end{aligned} \quad (36)$$

By comparing Eqs. (35) and (36) it may be concluded that:

$$\bar{T}_{IJ} = T_{IJ} + t_{IJ} \quad (37)$$

By substituting the Eq. (28), the third equation of (29), and Eq. (37) into the first equation of (31), the incremental equation of motion is obtained as:

$$(t_{IJ} + t_{JK}U_{I,K} + T_{JK}u_{I,K})_{,J} + \rho_0 b_J = \rho_0 \ddot{u}_I, \quad (38)$$

As it can be seen in Eq. (38), the initial stress bias and displacement gradient appear in the incremental equation of motion. Thus, the frequency response of the piezoelectric material will be affected by the initial thermo-electromechanical biases. To obtain the incremental electric displacement, the initial electric displacement is subtracted from the final electric displacement. The incremental electric displacement is obtained as:

$$d_p = \left[e_{LJP} + \frac{1}{2} \frac{\partial e_{LJP}}{\partial \theta} \times (\theta - \theta_0) - d_{LJKLP} \times S_{KL} + b_{LJPQ} \times W_Q \right] \times S_{KL} + \left[\varepsilon_{PQ} + \frac{\partial \varepsilon_{PQ}}{\partial \theta} \times (\theta - \theta_0) + \varepsilon_{PQR} W_R + b_{LJPQ} \times S_{KL} \right] W_Q \quad (39)$$

In a similar manner, for the boundary conditions, we obtain:

$$N_J (t_{JI} + t_{JK} U_{I,K} + T_{JK} u_{I,K}) = \tau_I^M \quad \text{on S} \quad (40)$$

$$\sigma = N_p d_p \quad \text{on S}$$

where, σ is the incremental surface charge density. Finally, by substituting fourth equation of (29) into the second equation of (32), the incremental charge equation is obtained:

$$d_{p,p} = 0 \quad (41)$$

The Eqs. (33), (36), (38), (39), (40), and (41) are the three dimensional governing equations and boundary conditions for the incremental fields. By solving these equations, the frequency shift in piezoelectric resonators due to finite initial biases is obtained.

4 RESULTS AND DISCUSSION

The derived equations for the initial and incremental fields in resonators enable us to simulate the force and temperature frequency effects in quartz resonators. The change in the resonance frequency of quartz resonators resulted from the change in the temperature, and insertion of the diametrical forces are referred to as the temperature frequency and force frequency effects [17]. These effects may lead to the frequency instabilities in the quartz resonators [1]. Researchers have measured the temperature frequency and force frequency effects in quartz [15, 21].

4.1 Finite element simulation procedure

In this research the multi-physics software COMSOL was used for the finite element modelling of the abovementioned effects in the resonator. This software gives the user the required flexibility to write his/her own partial differential equations and modify the equation of motion [1]. Since the quartz crystal has anisotropic characteristics, and its governing equations are nonlinear, the default feature of the FEA software cannot be employed. Therefore, the extracted nonlinear equations of the initial and the incremental models were converted to weak form expressions, and were assembled in the software environment to run sequentially. We used global variables (displacement gradient $U_{i,j}$, initial Strain, S_{ij} , and initial stress T_{ij}) to link the initial model to the incremental model in the resonance domain. This provides a one-way bridge of information to solve the initial and incremental models in sequence [22].

The finite element model includes two sub-models, the initial model and the incremental model. These two sub-models link three distinct sequential states of the quartz resonator. By employing the Lagrangian formulation, the displacements of all three states are referred to a single reference frame corresponding to the natural state of the resonator.

The initial model solves for the displacement, strain, and stress due to the external thermal or mechanical loading of the resonator. This model does not, however, contain the frequency response due to piezo electrically driven vibrations, so no piezoelectric factor is included in the initial model. The initial stresses, strains, and displacements,

which can be derived by the stationary study of quartz in the initial model, are considered as the incremental model inputs.

The incremental model solves for the incremental response of the resonator, including only the displacement, strain, and stress of piezoelectric vibrations. The final state of the resonator is then defined as the superposition of the initial and incremental response of the resonator [23]. Eigen-frequency investigation in the incremental model was considered to be harmonic. Hence, the motion equation takes the form of:

$$\begin{aligned} u_I &= \bar{u}_I e^{-I\omega t} \\ \rho_0 \omega^2 \bar{u}_I &= \left(t_{IJ} + t_{JK} U_{I,K} + T_{JK} u_{I,K} \right)_{,J} \quad \text{in } V \end{aligned} \quad (42)$$

where, ω is the resonance frequency. As seen, the initial displacement gradients and stresses are appeared in Eq. (42). In this paper, the AT-Cut quartz resonators have been selected for the model. AT-Cut quartz crystal is anisotropic, and it has monoclinic crystallographic system. AT-Cut of quartz is obtained by rotating Y-cut of quartz about x_1 axis by the angle of 35.25° [1].

The material constants of quartz, including second order elastic constants and their temperature derivatives [1], third order elastic constants [1, 24], second and third order dielectric permittivity piezoelectric constants [1, 25], thermoelastic constants [1], electro elastic constants [26] and Electrostrictive constants [25] are employed in the numerical model. It should be noted that the electro elastic tensor was implemented using extended partially symmetric tensor proposed by Kittinger [26]. This partially symmetric tensor includes 20 independent electro elastic coefficients. In the published literature, when the constants were measured for alpha quartz, the constants are changed under rotation of the axis for AT-Cut quartz crystal. All the calculated constants are applied in the finite element model to simulate the force and temperature frequency effects in AT-Cut quartz.

4.2 Response of quartz resonator to thermal biases (temperature-frequency effect)

As mentioned before, AT-cut quartz crystals are less sensitive to temperature around room temperature compared to other cuts of quartz. In this part, the temperature frequency behavior of AT-cut quartz crystals are investigated, and the simulation results are compared with the available experimental results [10]. According to Lee and Yong [10], we investigate a square blank of AT-cut quartz with resonance frequency of 10 MHz and thickness of 0.1660 mm in temperature range of 25°C to 100°C. The biasing thermal strains are simulated by the initial model. Then, according to the proposed model, the resultant stresses, strains, and displacement gradients are used as the incremental model input values. Finally, the Eigen-frequency investigation is performed under the initial temperature biases. The final results are shown in Fig. 3. As it can be observed, the FEM results using the nonlinear formulation are in good agreement with the Yong and Lee results.

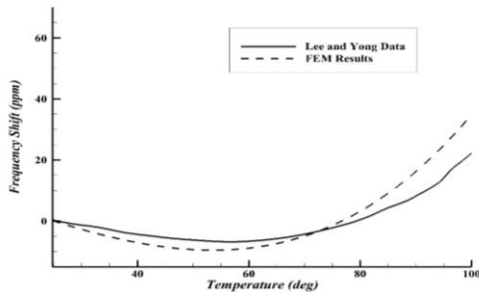


Fig.3
Temperature frequency effect in an AT-Cut quartz resonator.

4.3 Response of quartz resonators to thermo-mechanical biases (force-frequency effect at various temperatures)

The application of diametric forces causes initial static bias on the crystal, and changes the resonance frequency of quartz. This effect has been quantified by force frequency coefficient (K_f). The force frequency coefficient is calculated by: [27]

$$\frac{\Delta f}{f_0} = K_f \frac{FN_0}{Dt} \tag{43}$$

where, F is the applied force, $\Delta f / f_0$ is the fractional frequency shift, N is the frequency constant, D is the plate diameter, and t is the plate thickness. EerrNisse [21] measured the force frequency coefficient of AT-Cut quartz crystals at 25°C and 78°C as a function of force azimuth angle λ (see Fig. 4). His measurements showed that the force frequency coefficients are temperature dependent. The nonlinear equations extracted in this research include both the thermal and mechanical biases. Thus, this model is able to calculate the force frequency constants at various temperatures. To calculate the force frequency effect at different temperatures, all the material constants should be temperature dependent. In addition, the thermal biases should be considered.

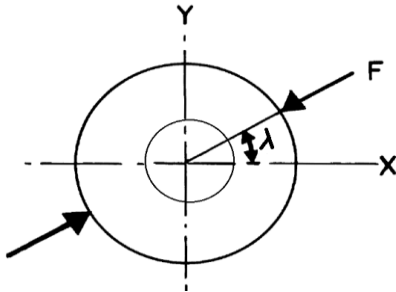


Fig.4 Circular quartz disc subjected to two opposed diametric forces.

We considered a circular AT-cut quartz disc with diameter of 10 mm, thickness of 0.1660 mm, and the fundamental first thickness shear frequency of 10 MHz, subjected to two 1N diametrically opposed forces. To calculate the force frequency constants at room temperature, at first, the crystal was considered to be in the natural state without any biasing deformations, and the natural thickness shear frequency (f_0 in Eq. (43)) is obtained. Then, the loads are applied diametrically to the crystal by angle λ that causes biasing mechanical deformations which are simulated by the initial model to calculate the initial displacement gradients and stresses. These displacement gradients and stresses are used as the input values for the incremental model. Finally, the Eq. (42) is solved in the incremental model, and the eigen frequencies are obtained. The calculated force frequency coefficients are shown in Fig. 5, along with the experimental data. The final finite element model involved 3124 Lagrangian quadratic elements, including 1246 boundary elements.

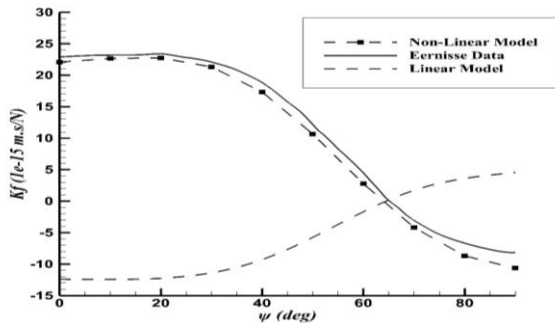


Fig.5 Force frequency curve for AT-Cut quartz resonator at 25°C.

For further analyzing the effect of the third order fundamental constants on the force frequency model, we neglected the nonlinear parts of the constitutive equations. Then, the force frequency coefficients were calculated with a linear model. The result is presented in Fig. 5. As shown, the nonlinearity has a considerable effect on the accuracy of the model.

The calculation of the force frequency coefficients at 78°C is performed for the first time in this paper. In this condition, the resonator undergoes both thermal and mechanical biases. Based on the force frequency experiments, it is assumed that the resonator undergoes a homogenous thermal bias due to the temperature increase. Then, by application of the mechanical loads, the frequency of the resonator is changed. The results concerning this condition are presented in Fig. 6.

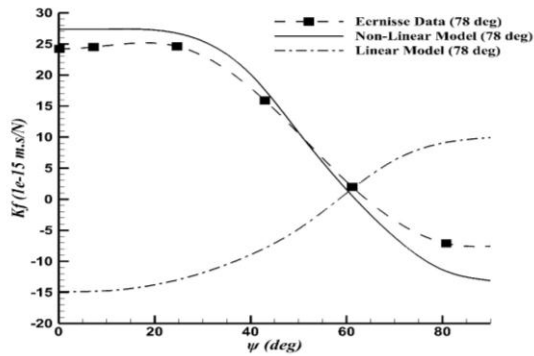


Fig.6
Force frequency curve for AT-Cut quartz resonator at 78°C.

To show the impact of nonlinear material constants on the calculations, all the nonlinear constants in the governing equations of the initial and incremental models, are considered to be zero. The results are illustrated in Fig. 6. As seen, the nonlinear model yields more accurate and realistic results.

5 CONCLUSIONS

In this paper, the governing nonlinear equations for the thermo-electro-elastic body under biasing fields were extracted. In the extraction of the nonlinear equations, the nonlinear Lagrangian strain and the second Piola-Kirchhoff stress tensors were used. The material was considered to have anisotropic characteristics. Also, the material can have piezoelectric and pyroelectric characteristics with arbitrary crystallographic symmetry. By defining suitable forms of the third order Gibbs electric energy, the fundamental linear and nonlinear material constants and their temperature derivatives were defined. Accordingly, the second Piola-Kirchhoff stress tensors, electric polarization vector, electric displacement vector, and entropy per unit mass, were defined. By using these equations, the governing equations for the incremental fields superposed on finite thermo-electromechanical biasing fields in piezoelectric resonators were derived. On this basis, the thickness shear vibrations of quartz resonators under thermal and mechanical and thermo-mechanical biasing fields were analyzed numerically. The results verified the effectiveness of the extracted nonlinear equations in analyzing the nonlinear nature of the temperature and force frequency effects in the piezoelectric resonators. The approach, methodology and results of this research assist in better understanding of quartz piezoelectric resonators. It is practically can be used for designing quartz resonator pressure sensors with more dependable accuracy and performance.

REFERENCES

- [1] Patel M. S., 2008, *Nonlinear Behavior in Quartz Resonators and its Stability*, PhD dissertation, New Brunswick, New Jersey University.
- [2] Ebrahimi F., Rastgoo A., 2009, Temperature effects on nonlinear vibration of FGM plates coupled with piezoelectric actuators, *Journal of Solid Mechanics* **1**(4): 271-288.
- [3] *Ultrasonics, Ferroelectrics, and Frequency Control*, 2015, IEEE Transactions on **62** **2015**(6): 1104-1113.
- [4] Baumhauer J. C., Tiersten H. F., 1973, Nonlinear electro elastic equations for small fields superposed on a bias, *The Journal of the Acoustical Society of America* **54**(4): 1017-1034.
- [5] Tichý J., Jiří E., Erwin K., Jana P., 2010, *Fundamentals of Piezoelectric Sensorics: Mechanical, Dielectric, and Thermodynamical Properties of Piezoelectric Materials*, Springer Science & Business Media.
- [6] Dulmet B., Roger B., 2001, Lagrangian effective material constants for the modeling of thermal behavior of acoustic waves in piezoelectric crystals. I. Theory, *The Journal of the Acoustical Society of America* **110**(4): 1792-1799.
- [7] Tiersten H. F., 1971, On the nonlinear equations of thermo-electro elasticity, *International Journal of Engineering Science* **9**(7): 587-604.
- [8] Tiersten H. F., 1975, Nonlinear electro elastic equations cubic in the small field variables, *The Journal of the Acoustical Society of America* **57**(3): 660-666.
- [9] Yang J. S., Batra R. C., 1995, Free vibrations of a linear thermo piezo electric body, *Journal of Thermal Stresses* **18**(2): 247-262.
- [10] Lee P. C. Y., Wang Y. S., Markenscoff X., 1975, High- frequency vibrations of crystal plates under initial stresses, *The Journal of the Acoustical Society of America* **57**(1): 95-105.

- [11] Lee P. C. Y., Yong Y. K., 1986, Frequency-temperature behavior of thickness vibrations of doubly rotated quartz plates affected by plate dimensions and orientations, *Journal of Applied Physics* **60**(7): 2327-2342.
- [12] Yong Y. K., Wu W., 2000, Lagrangian temperature coefficients of the piezoelectric stress constants and dielectric permittivity of quartz, *In Frequency Control Symposium and Exhibition, Proceedings of the 2000 IEEE/EIA International*.
- [13] *Ultrasonics, Ferroelectrics, and Frequency Control*, IEEE Transactions on 48 **2001**(5): 1471-1478.
- [14] Yong Y. K., Mihir P., Masako T., 2007, Effects of thermal stresses on the frequency-temperature behavior of piezoelectric resonators, *Journal of Thermal Stresses* **30**(6): 639-661.
- [15] Mase G., Thomas R., Smelser E., George E. M., 2009, *Continuum Mechanics for Engineers*, CRC press.
- [16] Lee P. C. Y., Yong Y. K., 1984, Temperature derivatives of elastic stiffness derived from the frequency-temperature behavior of quartz plates, *Journal of Applied Physics* **56**(5): 1514-1521.
- [17] Yang J., 2013, *Vibration of Piezoelectric Crystal Plates*, World Scientific.
- [18] Yang J., 2005, *An Introduction to the Theory of Piezoelectricity*, Springer Science & Business Media.
- [19] Kuang Zh. B., 2011, *Some Thermodynamic Problems in Continuum Mechanics*, INTECH Open Access Publisher.
- [20] Montanaro A., 2010, Some theorems of incremental thermo-electro elasticity, *Archives of Mechanics* **62**(1): 49-72.
- [21] Yang J., Yuantai H., 2004, Mechanics of electro elastic bodies under biasing fields, *Applied Mechanics Reviews* **57**(3): 173-189.
- [22] EerNisse E.P., 1980, Temperature dependence of the force frequency effect for the AT, FC, SC and rotated X-Cuts, *34th Proceedings of the Annual Symposium on Frequency Control*.
- [23] Beerwinkle A. D., 2011, *Nonlinear Finite Element Modeling of Quartz Crystal Resonators*, M.S. Thesis, Oklahoma State University, Stillwater, USA.
- [24] Mohammadi M. M., Hamed M., 2016, Experimental and numerical investigation of force-frequency effect in crystal resonators, *Journal of Vibro-Engineering* **18**(6): 3709-3718.
- [25] Thurston R. N., McSkimin H. J., Andreatch Jr P., 1966, Third-order elastic coefficients of quartz, *Journal of Applied Physics* **37**(1): 267-275.
- [26] Kittinger E., Jan T., Wolfgang F., 1986, Nonlinear piezoelectricity and electrostriction of alpha quartz, *Journal of Applied Physics* **60**(4): 1465-1471.
- [27] Reider Georg A., Erwin K., Tichý J., 1982, Electro elastic effect in alpha quartz, *Journal of Applied Physics* **53**(12): 8716-8721.
- [28] Ratajski J. M., 1968, Force-frequency coefficient of singly rotated vibrating quartz crystals, *IBM Journal of Research and Development* **12**(1): 92-99.